ARCHIVES
OF THERMODYNAMICS

Comparative thermo-hydraulic analysis of periodic stepped open micro pin-fin heat sink

Prabhakar Bhandari[a*], Bhavesh Vyas[b], Diwakar Padalia[c], Lalit Ranakoti[d], Yogesh Kumar Prajapati[e], Raghubeer Singh Bangari[f]

[a]Department of Mechanical Engineering, School of Engineering and Technology, K. R. Mangalam University, Gurugram-122103, Haryana, India
[b]Department of Electrical and Electronics Engineering, School of Engineering and Technology, K. R. Mangalam University, Gurugram-122103, Haryana, India
[c]Department of Physics, School of Basic and Applied Sciences, K. R. Mangalam University, Gurugram-122103, Haryana, India
[d]Department of Mechanical Engineering, Graphic Era Deemed to Be University, Dehradun-248002, Uttarakhand, India
[e]Department of Mechanical Engineering, BIT Sindri, Dhanbad-828123, Jharkhand, India
[f]Department of Mechanical Engineering, Graphic Era Hill University, Dehradun-248002, Uttarakhand, India
*Corresponding author email: prabhakar.bhandari40@gmail.com

Abstract

There is no doubt that the miniaturization of various electronic devices, including processors, servers, micro-electromechanical system devices, etc. has resulted in increased overall performance. However, there is a major problem with thermal management in these devices, as well as in many others. One of the most promising solutions is liquid cooled microchannel heat sink. In the current work, different cases of open micro pin-fin configurations of heat sink were considered. The configurations considered were a uniform height micro pin-fin heat sink, three-stepped unidirectional micro pin-fin heat sink and three-stepped bi-directional micro pin-fin heat sink. These configurations were also oriented in two dissimilar fashions, i.e. inline and staggered, so the total of six heat sink configurations are compared and analysed. Using single phase water as a coolant and copper as a substrate, these configurations were simulated numerically for different Reynolds numbers (10−160) under heat flux of 500 kW/m^2. It can be concluded that at low Reynolds numbers, steepness does not contribute much in both inline and staggered arrangements, while at higher Reynolds numbers, 3 stepped staggered configurations has revealed the best performance due to boosted fluid mixing and more projecting secondary flow. Furthermore, bi-directionality in steepness shows augmented performance only in inline arrangement.

1. Introduction

The trend of miniaturization has led to the increased generation of heat flux in many engineering devices, such as electronic chips and micro electromechanical systems. It is certain that it will reach 10 000 kW/m^2 in the immediate future [1]. It is possible for such devices to fail permanently if heat generation is not properly managed. This quantity of heat cannot be removed

Bhandari P., Vyas B., Padalia D., Ranakoti L., Prajapati Y.K., Bangari R.S.

Nomenclature

A – area, mm^2
c_p – specific heat, J/(kg·K)
D_h – hydraulic diameter, mm
H – height, mm
k – thermal conductivity, W/(m·K)
L – length, mm
N – total number of pin fins
$\overline{Nu}$ – average Nusselt number
Δp – pressure drop, Pa
q – heat flux, kW/m^2
Re – Reynolds number
T – temperature, K
$\overline{T_{bw}}$ – average bottom wall temperature, K
TPF – thermal performance factor
U – velocity, m/s
V – velocity matrix, m/s
W – width, mm

Greek symbols
μ – dynamic viscosity, Pa·s

ρ – density, kg/m^3

Subscripts and Superscripts
avg – average
b – bottom
$bulk$ – bulk fluid
ch – channel
eff – effective
f – fin
in – inlet
l – liquid
o – base configuration
s – substrate
wl – solid liquid interface

Abbreviations and Acronyms
HS – heat sink
MCHS – microchannel heat sink
MEMS – micro-electromechanical system
MPFHS – micro pin fin heat sink
STEP – stepped
UO – uniform

by natural or forced air convection, and a better cooling system is necessary [2].

Micro heat pipes, jet impingement, thermoelectric, carbon nanotubes, spray cooling, and microchannels have proven capable of dissipating an enormous amount of heat [3, 4], and due to its ease of application and smaller coolant volume requirement, microchannel heat sinks (MCHS) have gained extensive popularity in the research fraternity.

Since Tuckerman and Pease [5] implemented microchannels for cooling electronic circuits, various approaches have been used to enhance the cooling performance. A number of external factors, such as vibrations, electric fields, magnetic fields, etc. are used to enhance the performance of MCHS in active techniques [6]. In passive techniques, the innovative geometry of the heat sink and various working fluids have been used to increase performance [7]. Working fluid modification such as nanofluids, phase change material slurries [8,9], and the use of multiphase approach [10] has been more extensively studied, while some innovative designs built into the microchannel are multilayer microchannels, the use of vortex generator in the microchannel, multiple bifurcation, pin-fin arrangement, etc. [6]. The main idea behind using these geometrical altercations is enhanced wetted surface area, i.e. convective area, and better fluid mixing.

Generally, micro pin-fin heat sink (MPFHS) is having pin fin height equivalent to the channel height and termed as closed MPFHS. Next, it was proposed to keep the fins' height lesser than the channel height to achieve the clearance. In order to improve thermal performance, the pin fin tip clearance should be between 20% and 25% of channel height [6]. The same range of tip clearance was also proven through experimental work [11]. It was observed that a larger tip clearance results in lesser convective area while a smaller tip clearance does offers better flow mixing. To further augment the heat transfer capacity, Bhandari

and Prajapati [12, 13] opted for a stepped arrangement of MPFHS, replacing the uniform tip clearance arrangement. They found that the pin fin in step size of three rows has yielded better results compared to two and four pin fin rows. They also pointed out that increasing the tip clearance along the flow direction has a better performance than the decreasing pattern. Earlier the stepped arrangement was considered only along the microchannel length direction. To further increase the fluid mixing, Bhandari [14] opted for a stepped arrangement along both the microchannel length and microchannel width directions. The development of stepness in MPFHS is shown in Fig. 1.
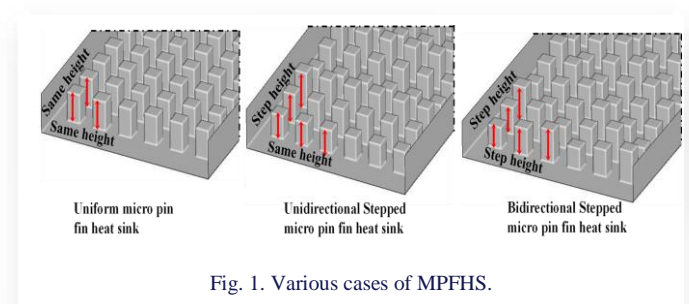

Fig. 1. Various cases of MPFHS.

Two dissimilar pin-fin arrangements, i.e. inline and staggered were often considered in MPFHS designs. An experimental comparison [15] revealed that staggered configurations possess greater heat transfer coefficients and friction factors compared to inline arrangements under similar flow rates and packaging densities. However, prevailing differences in performance diminish with the increasing packaging density. Keshavarz et al. [16] examined the performance of circular and drop shaped MPFHS having inline and staggered arrangements. The authors perceived that the staggered arrangement has a higher outlet temperature for lesser fin density, while the inline arrangement has more outlet temperature for moderate pin-fin density. However, for all pin-fin density configurations, the

staggered arrangement has a higher pressure drop compared to the inline arrangement. In recent work by Bhandari et al. [17], different pin fin shapes were analyzed. They found that four-side arrangements have the best performance among different cases. The fluid flow mixing is one of the important factors that affects the thermo-hydraulic performance [18].

The micro pin fin heat sink represents a crucial innovation with diverse applications across several domains [19−21]. Primarily, it plays a pivotal role in battery thermal management systems, ensuring the efficient dissipation of heat generated during charging and discharging processes. This is particularly relevant in the context of advancing battery technologies, where effective thermal control is imperative for enhancing overall performance and longevity. Moreover, the utilization of micro pin fin heat sinks extends to hydrogen storage systems, contributing to the optimal management of thermal conditions in the storage process. In the realm of solar photovoltaic (PV) technology, these heat sinks find application in cooling systems, addressing the challenge of excess heat accumulation during solar energy conversion [22−26]. Additionally, in electronics cooling, microchannel heat sinks play a vital role in addressing thermal challenges associated with modern, compact electronic devices, enhancing their reliability and longevity [27, 28]. This underscores the versatility of micro pin fin heat sinks in facilitating enhanced thermal regulation across diverse technological domains. Recent advancements in materials and design methodologies further underscore the ongoing development in this field, emphasizing the contemporary relevance of micro pin fin heat sinks in addressing evolving thermal management needs.

In the present work, the directionality of stepped MPFHS configurations has been numerically studied in two different fashions. The total of six different configurations have been compared on the basis of the average Nusselt number ($\overline{Nu}$), pressure drop (Δp) and thermal performance factor (*TPF*). It is the primary objective of the existing work to investigate out-of-plane mixing in MPFHS.

2. Mathematical modelling

2.1. Heat sink geometry

A numerical analysis of different MPFHS configurations is carried out in the present work. The total of six MPSHS configurations were chosen, including three in inline arrangement and the others in staggered arrangement. All MPFHS geometrical constructions are as follows:

1) Uniform inline MPFHS (UO inline): In this configuration, pin fins have uniform height throughout the heat sink length and width. Pin fin height of 0.375 mm is kept in channel of height 0.5 mm. Further, fins are arranged in inline style. This configuration is kept as a base configuration to assess the total performance of modified sinks.
2) Uniform staggered MPFHS (UO stagerred): A staggered arrangement of pin-fins in this configuration is characterized by equal height and even spacing.
3) Three-stepped inline unidirectional MPFHS (3 step inline): The pin-fin height differs in three consecutive rows, i.e. along the channel length only.

4) Three-stepped staggered unidirectional MPFHS (3 step staggered): Similar configuration as described in (c) but arranged in staggered fashion.
5) Three-stepped inline bidirectional MPFHS (3 × 3 step inline): Pin-fin height variation takes place along both longitudinal direction and transverse direction in inline fashion.
6) Three-stepped staggered bidirectional MPFHS (3 × 3 step staggered): Similar to 5), but arranged in staggered fashion. The perspective view and top view of 3 × 3 step staggered configuration are depicted in Fig. 2.

(a)   (b)

Fig. 2. Three-stepped staggered bidirectional MPFHS
(3 × 3 step staggered): (a) Perspective view; (b) Top view
with its geometrical specification in mm.
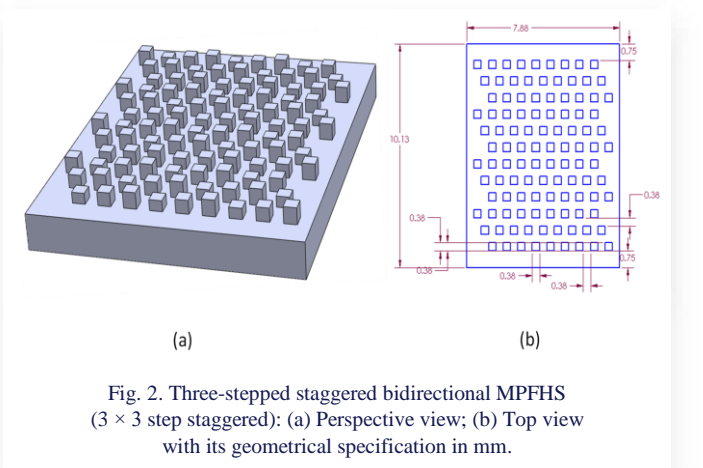
As depicted above, a 3-D model of the heat sinks (HS) has been designed to conduct the current simulation work. The footprint area and overall height of the considered cases are equal, namely 10.13 × 7.875 × 1.5 mm. In all cases, pin fins have a square cross section, which measures 0.375 mm by 0.375 mm. The pin fins are positioned differently across nine columns, each with twelve fins along the channel length. So, the total of 108 pin fins are there in every heat sink. The thorough geometrical specifications of the open MPFHS are tabulated in Table 1.

Table 1. MPFHS geometrical specifications.

Parameter	Value (mm)
MPFHS length (*L*)	10.125
MPFHS width (*W*)	7.875
Micro Fin height variation (H_f)	300−375−450
total height of Heat sink ($H = H_{ch}+H_b$)	1.5
Bottom wall thickness (H_b)	1
Footprint dimension of fin (W_f)	0.375×0.375
Pitch between two successive pin-fins along channel length	0.375
Pitch between two successive pin-fins along channel width	0.375
Total fins in each configuration	108

2.2. Solution methodology

Fluid flow and thermal characteristics of projected MPFHS cases under different flow rates were examined using the same operating conditions. Simulations were performed using ANSYS Fluent Version 18.0 commercial code to study the different

heat sink geometries, where geometry and meshing have been carried out in Workbench. Copper is the substrate of the heat sink, while liquid water is the coolant.

The steady-state basic governing equations, i.e. continuity Eq. (1), momentum Eq. (2), and energy Eq. (3) applicable for the fluid flow zone are:

$$\nabla \cdot \left(\rho_l \vec{V} \right) = 0, \tag{1}$$

$$\vec{V} \cdot \nabla \left(\rho_l \vec{V} \right) = -\nabla p + \nabla \cdot \left(\mu_l \nabla \vec{V} \right) + \rho_l \vec{g}, \tag{2}$$

$$\vec{V} \cdot \nabla \left(\rho_l\, c_{p,l} \nabla T_l \right) = \nabla \cdot \left(k_l\, \nabla T_l \right). \tag{3}$$

In the above equations $\vec{V}$ is the velocity matrix. The energy equation for solid substrates is:

$$\nabla \cdot \left(k_s\, \nabla T_s \right) = 0. \tag{4}$$

The thermo-physical properties of single phase liquid water vary with temperature. For more accurate results, the same has also been incorporated into the simulation. The variation of liquid thermophysical properties is a polynomial function of temperature [28, 30], while the substrate material has constant properties. Both properties of substrate and working fluid are listed in Table 2.

Table 2. Thermo-physical property of substrate material and working fluid.

Thermo-physical property	Copper	Working fluid (Water)
Density	8978 kg/m³	$\rho(T) = 765.33 + 1.8142\,T - 0.0035\,T^2$
Specific heat	381 J/(Kg·K)	$c_p(T) = 28070 - 281.7\,T + 1.25\,T^2 - (2.48 \times 10^{-3})\,T^3 + (1.857 \times 10^{-6})\,T^4$
Thermal conductivity	387.6 W/(m·K)	$k(T) = -0.5752 + (6.397 \times 10^{-3})\,T - (8.151 \times 10^{-6})\,T^2$
Viscosity	------	$\mu(T) = (9.67 \times 10^{-2}) - (8.207 \times 10^{-4})\,T + (2.344 \times 10^{-6})\,T^2 - (2.244 \times 10^{-9})\,T^3$

The pressure drop was evaluated as a pressure difference between the inlet and outlet. The Reynolds number (Re) was calculated based on the heat sink pin fin hydraulic diameter according to:

$$\mathrm{Re} = \frac{\rho u_{in} D_h}{\mu}. \tag{5}$$

Based on the expression below, the average Nusselt number $\overline{\mathrm{Nu}}$ has been calculated

$$\overline{\mathrm{Nu}} = \frac{h D_h}{k_l} = \frac{q_{eff} D_h}{(T_{avg,wl} - T_{bulk,l}) k_l}, \tag{6}$$

where, the area weighted average temperature of the heat sink's s-l interface is $T_{avg,wl}$. $T_{bulk,l}$ is the bulk volumetric working fluid temperature. As the wetted surface area is greater than the foot print area, the effective heat flux (q_{eff}) has been opted in $\overline{\mathrm{Nu}}$.

The effective heat flux is the heat flux applied on the interface and has been evaluated according to Eq. (7):

$$q_{eff} = \frac{A_{bw}}{A_{wl}}, \tag{7}$$

where A_{bw} and A_{wl} refer to the bottom wall surface area or footprint area and the solid-liquid contact area of the heat sink, respectively. Regardless of the configuration, both areas remain the same.

2.3. Boundary conditions

In current numerical work, a uniform heat flux of 500 kW/m² has been applied. Previous studies [6,11] have shown that the heat flux has little influence on microchannel heat sink properties. So, only one heat flux condition has been studied. Except for the bottom wall, all outer walls are adiabatic. Working fluid with a temperature of 298 K was taken with inlet velocity varying from 0.1 to 0.4 m/s. Pressure–velocity coupling was based on the SIMPLE algorithm, and the equations were solved using the Gauss-Seidel iterative technique.

2.4. Grid independence

In order to prevent any errors resulting from coarse mesh, a grid independence test was performed before the broad analysis. The uniform inline (UO) MPFHS case having unit grid size variation was considered. In total, three different cases were simulated with Re = 110 and q = 500 kW/m². Table 3 enlists the complete details of the grid independence test. Two parameters − pressure drop (Δp) and average bottom wall temperature ($\overline{T}_{bw}$) were compared for a varying number of elements. It is observed that the differences in results for fine and very fine grid structures are less than 3%, but time taken for the simulation is doubled. So, the fine mesh type is chosen in simulation of all MPFHS cases.

Table 3. Grid independence test performed on uniform inline (UO) configuration for Re = 110.

Mesh Type	Number of elements	Pressure drop	Percentage variation
Coarse	256 849	430.846	--
Fine	1 994 845	458.4352	6.40%
Very Fine	4 674 104	467.694	2.01%
Mesh Type	Average bottom wall temperature	Percentage variation	
Coarse	335.6415	--	
Fine	333.6879	0.58%	
Very Fine	332.8774	0.24%	

2.5. Model validation

Using the methodologies of the proposed model, the work of Ali and Arshad [29] has been reproduced to validate the present numerical work. Identical boundary conditions and similar micro pin fin geometry have been used to predict the results. Under a heat flux of 37.2 kW/m², the bottom wall temperature was compared for different flow rates. Furthermore, it is compared

to the numerical work by Ambreen and Kim [30], as they have also used a similar geometry [29]. Based on the present simulation and the literatures, the predicted average bottom wall temperature is shown in Fig. 3. Observations of the present results show decent agreement with both literatures, with an extreme deviation of 5%.
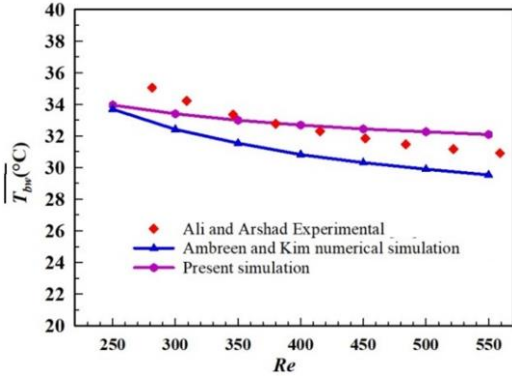

Fig. 3. Present numerical work validation with previous work [29−30].

3. Results and discussion

On simulating different heat sink configurations under heat flux of 500 kW/m^2, the parameters $\overline{Nu}$ and $\overline{T}_{bw}$ were evaluated for a series of Reynold numbers (Re). The variation of $\overline{Nu}$ with Re for different MPFHS cases has been shown in Fig. 4(a). As depicted in the figure, with a rise in Re, there is a rise in $\overline{Nu}$ value but with a decreasing rate. This can be attributed to an increase in entrance length. There is a distinct gap between inline and staggered configurations for all heat sinks, which is quite obvious due to enhanced fluid mixing. It is exciting to note that for inline configurations, 3 × 3 step MPFHS has shown top performance followed by 3 step inline and UO inline configuration. While, for staggered configurations, the differentiation is not clearly visible up to Re < 70, and afterwards, 3 step (staggered) configuration has yielded a better $\overline{Nu}$ value compared to 3 × 3 step (staggered) and UO (staggered) configuration. The observed conduct is entirely contingent on how the working fluid moves within the heat sink.

The influence of Reynolds number (Re) on the average temperature of the bottom wall ($\overline{T}_{bw}$) was illustrated in Fig. 4(b) for different cases of the heat sink.
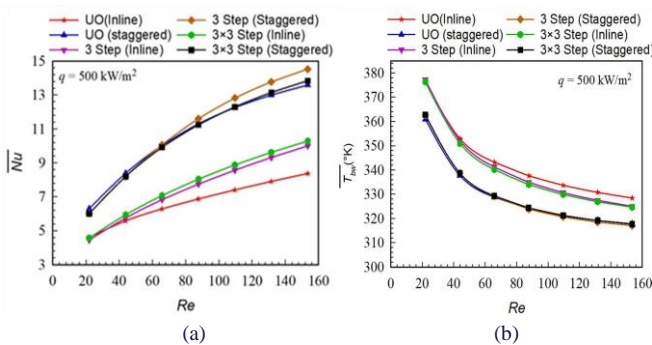

Fig. 4. Deviation of: (a) $\overline{Nu}$; (b) $\overline{T}_{bw}$ with Re for different MPFHS configuration.

The average bottom wall temperature $\overline{T}_{bw}$ is calculated as the area-weighted normal temperature of the lower wall of the heat sink where the heat flux is applied. Across various configurations of the heat sink, a consistent trend in the bottom wall temperature with respect to Reynolds number was observed. The general understanding is that as the Reynolds number increases, the coolant flow rate also increases, leading to more effective heat transfer from the heat sink and a decreased bottom wall heat sink temperature. A significant difference was observed between inline and staggered arrangements due to better fluid flow through the channel. Among all configurations, 3 step (staggered) configuration has shown the lowest value of $\overline{T}_{bw}$ for Re > 70 and for Re < 70; it is UO staggered configuration. This is due to a higher heat transfer rate in this case. It can be concluded that heat sink usage at low Reynold numbers is not justified as there is less heat transfer than.

The variation of Δp with Re for different MPFHS cases has been plotted in Fig. 5(a). It is recognized that as Re increases, there is a corresponding rise in the pressure drop (Δp) due to elevated flow resistance. Additionally, the gradient of the Δp curve becomes steeper as the Reynolds number value increases. Among different configurations, 3 step staggered configuration has yielded highest value of pressure drop, while UO inline configuration has shown the lowest Δp. This is due to increase in flow obstruction in the heat sink. The gap between inline and staggered arrangements kept on increasing with the rise in Re.

To further evaluate the design efficacy of heat sinks, the thermal performance factor (*TPF*) was plotted in Fig. 5(b). The enhancement of the average Nusselt number through diverse design modifications invariably involves incurring a pressure drop penalty [22]. Consequently, researchers have endeavored to assess the effectiveness of these designs using various parameters such as thermo-hydraulic performance, figure of merit, and coefficient of performance [22,31−33]. In the current study, the overall performance of various heat sink configurations was evaluated based on the parameter *TPF*. The thermal performance factor based on Eq. (8) has been calculated to assess the overall performance of MPFHS configurations.
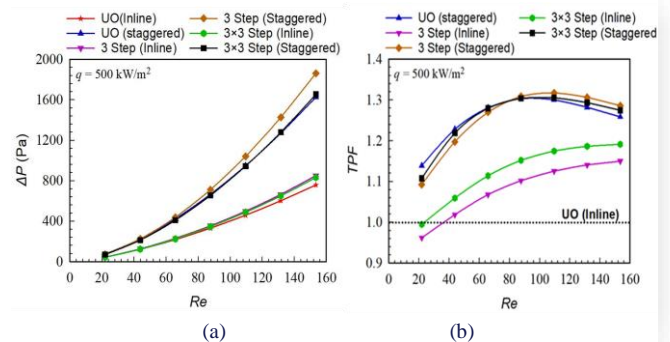

Fig. 5. Deviation of: (a) Δp; (b) *TPF* with Re.

All configurations have shown the *TPF* value > 1 except at lower values of Re. The design modifications have augmented thermal characteristics with the least pressure drop penalty. Among all configurations, UO stepped configuration has the

maximum value of *TPF* up to Re < 80, while for Re > 80, 3 step staggered configuration has depicted the highest *TPF* value.

The TPF value for UO stepped, 3 step staggered and 3 × 3 step staggered configurations of MPFHS has shown an increasing trend up to Re = 80 and afterwards it starts decreasing. This is attributed to exponential enhancement in pumping power at higher Re values. Whereas, the other configurations, i.e. 3 step inline and 3 × 3 step inline have shown an increasing slope with the increase in Reynolds number, and at higher Re values, the curves tend to flatten.

4. Conclusions

In current work, numerical relative analysis has been done for different configurations of open MPFHS. Mainly three design parameters (stepness, arrangement and directionality) are simulated and analysed using six different MPFHS configurations. Using single phase liquid water as a coolant and Cu as a substrate, present cases were compared for a range of Reynolds number and a heat flux of 500 kW/m². It can be concluded that stepness in pin fin configurations has yielded more augmentation in the inline arrangement rather than in the staggered arrangement. Furthermore, the stepped arrangement has less impact at low values of Reynolds number, i.e. for Re < 70, its influence kept on increasing with Re. Bi-directional pin fin height variation is beneficial only in the inline arrangement while has a negative impact on the staggered arrangement.

Acknowledgements

References

[1] Lee, J., & Mudawar, I. (2009). Low-temperature two-phase micro-channel cooling for high-heat-flux thermal management of defense electronics. *IEEE Transactions on Components Packaging and Manufacturing Technology*, 32(2), 453–465. doi: 10.1109/ITHERM.2008.4544263

[2] Ahmed, H.E., Salman, B.H., Kherbeet, A.S., & Ahmed, M.I. (2018). Optimization of thermal design of heat sinks: A review. *International Journal of Heat and Mass Transfer*, 118, 129–153. doi: 1016/j.ijheatmasstransfer.2017.10.099

[3] Kandlikar, S.G., & Bapat, A.V. (2007). Evaluation of jet impingement, spray and microchannel chip cooling options for high heat flux removal. *Heat Transfer Engineering*, 28(11), 911–923. doi: 10.1080/01457630701421703

[4] Gururatana, S. (2012). Heat transfer augmentation for electronic cooling. *American Journal of Applied Sciences*, 9(3), 436–439. doi: 10.3844/ajassp.2012.436.439

[5] Tuckerman, D.B., & Pease, R.F.W. (1981). High-performance heat sinking for VLSI. *IEEE Electron Device Letters*, 2(5), 126–129. doi: 10.1109/EDL.1981.25367

[6] Bhandari, P., & Prajapati, Y.K. (2021). Thermal performance of open microchannel heat sink with variable pin fin height. *International Journal of Thermal Sciences*, 159, 106609. doi: 10.1016/j.ijthermalsci.2020.106609

[7] Bhandari, P., Singh, J., Kumar, K., & Ranakoti, L. (2022). A review on active techniques in microchannel heat sink for miniaturization problem in electronic industry. *Acta Innovations*, 45, 45-54. doi: 10.32933/ActaInnovations.45.4

[8] Kumar, N., Singh, P., Redhewal, A.K., & Bhandari, P. (2015). A review on nanofluids applications for heat transfer in microchannels. *Procedia Engineering*, 127, 1197–1202. doi: 10.1016/ j.proeng.2015.11.461

[9] Rajabifar, B. (2015). Enhancement of the performance of a double-layered microchannel heat sink using PCM slurry and nanofluid coolants. *International Journal of Heat and Mass Transfer*, 88, 627–635. doi: 10.1016/j.ijheatmasstransfer.2015.05.007

[10] Bhandari, P., & Prajapati, Y.K. (2017). Flow boiling instabilities in microchannels and their promising solutions – A review. *Experimental Thermal and Fluid Science*, 88, 576-593. doi: 10.1016/j.expthermflusci.2017.04.014

[11] Bhandari, P., & Prajapati, Y.K. (2022). Influences of tip clearance on flow and heat transfer characteristics of open-type micro pin fin heat sink. *International Journal of Thermal Sciences*, 179, 107714. doi: 10.1016/j.ijthermalsci.2021.107714

[12] Bhandari, P., & Prajapati, Y.K. (2021). Fluid flow and heat transfer behavior in distinct array of stepped micro pin fin heat sink. *Journal of Enhanced Heat Transfer*, 28(4), 31–61. doi: 10.1615/JEnhHeatTransf.2021037008

[13] Bhandari, P., & Prajapati, Y.K. (2020). Numerical analysis of different arrangement of square pin-fin microchannel heat sink. In B. Biswal, B. Sarkar, & P. Mahanta (Eds.), *Advances in Mechanical Engineering, Lecture Notes in Mechanical Engineering* (pp. 879–891). Singapore: Springer. doi: 10.1007/978-981-15-0124-1_79

[14] Bhandari, P. (2022). Numerical investigations on the effect of multi-dimensional steepness in open micro pin fin heat sink using single-phase liquid fluid flow. *International Communications in Heat and Mass Transfer*, 138, 106392. doi: 10.1016/j.icheatmasstransfer.2022.106392

[15] Wirtz, R., & Colban, D.M. (1996). Comparison of the cooling performance of staggered and in-line arrays of electronic packages. *Journal of Electronic Packaging, Transactions of the ASME*, 118, 27–30. doi: 10.1115/1.2792123

[16] Keshavarz, A., Lavasani, M., & Bayat, H. (2019). Numerical analysis of effect of nanofluid and fin distribution density on thermal and hydraulic performance of a heat sink with drop-shaped micro pin fins. *Journal of Thermal Analysis and Calorimetry*, 135(2), 1211–1228. doi: 10.1007/s10973-018-7711-z

[17] Bhandari, P., Padalia, D., Ranakoti, L., Khargotra, R., András, K., & Singh, T. (Year). Thermo-hydraulic investigation of open micro prism pin fin heat sink having varying prism sides. *Alexandria Engineering Journal*, 69, 457-468. doi: 10.1016/j.aej.2023.02.016

[18] Bhandari, P., Rawat, K.S., Prajapati, Y.K., Padalia, D., Ranakoti, L., Singh, T., & Joshi, K. (2023). Design modifications in micro pin fin configuration of microchannel heat sink for single-phase liquid flow: A review. *Journal of Energy Storage*, 66, 107548. doi: 10.1016/j.est.2023.107548

[19] Kumari, N., Alam, T., Ali, M.A., Yadav, A.S., Gupta, N.K., Siddiqui, M.I.H., Dobrota, D., & Rotaru, I.M. (2022). Numerical investigation on hydrothermal performance of microchannel heat sink with periodic spatial modification on sidewalls. *Micromachines*, 13, 1986. doi: 10.3390/mi13111986

[20] Saha, S., Alam, T., Siddiqui, M.I.H., Kumar, M., Ali, M.A., Gupta, N.K., & Dobrota, D. (2022). Analysis of microchannel heat sink of silicon material with right triangular groove on side-wall of passage. *Materials*, 15, 7020. doi: 10.3390/ma15197020

[21] Vatsa, A., Alam, T., Siddiqui, M.I.H., Ali, M.A., & Dobrotă, D. (2022). Performance of microchannel heat sink made of silicon material with the two-sided wedge. *Materials*, 15(14), 4740. doi: 10.3390/ma15144740

[22] Bhandari, P., Rawat, K.S., Prajapati, Y.K., Padalia, D., Ranakoti, L., & Singh, T. (2023). A review on design alteration in micro-channel heat sink for augmented thermohydraulic performance. *Ain Shams Engineering Journal*, 15(2), 102417. doi: 10.1016/j.asej.2023.102417

[23] Dash, A.P., Prada, T., Alam, T., Siddiqui, M.I.H., Blecich, P., Kumar, M., Gupta, N.K., Ali, M.A., & Yadav, A.S. (2022). Impact on heat transfer rate due to an extended surface on the passage of microchannel using cylindrical ribs with varying sector angle. *Energies*, 15(21), 8191. doi: 10.3390/en15218191

[24] Bhandari, P., Prajapati, Y.K., & Uniyal, A. (2022). Influence of three-dimensionality effects on thermal hydraulic performance for stepped micro pin fin heat sink. *Meccanica*, 58, 2113-2129. doi: 10.1007/s11012-022-01534-4

[25] Bhandari, P., Kumar, K., Ranakoti, L., Bisht, V.S., Lila, M.K., Joshi, K., Raju, N.V.G., Sobti, R., & Jayahari, L. (2023). Thermo-hydraulic investigation of two stepped micro pin fin heat sink having variable step size. *E3S Web of Conferences*, 430, 01177. doi: 10.1051/e3sconf/202343001177

[26] Bhandari, P., Prajapati, Y.K., & Bisht, V.S. (2021). Heat transfer augmentation in micro pin fin heat sink using out of plane fluid mixing. In *Proceedings of the 26th National and 4th International ISHMT-ASTFE Heat and Mass Transfer Conference, IIT Madras* (pp. 1595–1600). Begel House Inc. doi: 10.1615/IH-MTC-2021.2400

[27] Bhandari, P., & Prajapati, Y.K. (2021). Experimental investigation of variable tip clearance in square pin fin microchannel heat sink. In *Proceedings of the 26th National and 4th International ISHMT-ASTFE Heat and Mass Transfer Conference, IIT Madras* (pp. 1351–1356). Begel House Inc. doi: 10.1615/IHMTC-2021.2040

[28] Bhandari, P., & Prajapati, Y.K. (2021). Numerical study of fluid flow and heat transfer in stepped micro-pin–fin heat sink. In T. Prabu, P. Viswanathan, A. Agrawal, & J. Banerjee (Eds.), *Fluid Mechanics and Fluid Power, Lecture Notes in Mechanical Engineering* (pp. 373–381). Springer. doi: 10.1007/978-981-16-0698-4_40

[29] Ali, H.M., & Arshad, W. (2015). Thermal performance investigation of staggered and inline pin in heat sinks using water-based rutile and anatase TiO$_2$ nanofluids. *Energy Conversion and Management*, 106, 793–803. doi: 10.1016/j.enconman.2015.10.015

[30] Ambreen, T., & Kim, M. (2018). Effect of fin shape on the thermal performance of nanofluid-cooled micro pin-fin heat sinks. *International Journal of Heat and Mass Transfer*, 126, 245–256. doi: 10.1016/j.ijheatmasstransfer.2018.05.164

[31] Ghildyal, A., Bisht, V.S., Rawat, K.S., & Bhandari, P. (2023). Effect of D-shaped, reverse D-shaped and U-shaped turbulators in solar air heater on thermohydraulic performance. *Archives of Thermodynamics*, 44(2), 3-20. doi: 10.24425/ather.2023.146556

[32] Thapa, R.K., Bisht, V.S., Rawat, K., & Bhandari, P. (2023). Computational analysis of automobile radiator roughened with rib roughness. *Journal of Heat and Mass Transfer Research*, 9, 209-218. doi: 10.22075/jhmtr.2023.27617.1382

[33] Karmveer, Gupta, N.K., Alam, T., & Singh, H. (2022). An experimental study of thermohydraulic performance of solar air heater having multiple open trapezoidal rib roughnesses. *Heat Transfer*, 1–21. doi: 10.1080/08916152.2022.2139024